relative humidity for equivalent exposure times. Average sulfate production for the carbon suspensions in the bubbler was 0.042 mg/m^2 h, while that for the initially dry particulates exposed to the flowing gas mixture was 0.051 mg/m^2 h. We feel that these values are in good agreement and demonstrated the significance of the role of carbon surface area on the conversion process. The production of sulfate (based on surface area) in the bubbler was lower than that on the particles, even though the NO_2 concentration in the bubbler was higher. Two simple observations are offered that may help to explain this result. The total mass (not concentration) of SO_2 available for oxidation per unit of carbon surface was lower in the bubbler experiment, and the ratio of liquid water to carbon surface was higher. Either, or both, of these conditions may have influenced sulfate production somewhat. Nevertheless, as noted, the agreement between the specific sulfate yields is quite good considering the significant differences in experimental techniques and conditions, and suggested that as long as sufficient H_2O is present to alleviate saturation, the transformation process will not be highly sensitive to bulk water concentrations. These results also suggest that the SO_2 transformation chemistry observed on the initially dry carbon particles, once "wetted" by contact with the 65% relative humidity air, behaved chemically as a carbon/water suspension.

Conclusions

The results of these experiments indicate that graphitic carbon particles effectively catalyze the oxidation of SO_2 to sulfate by NO_2 in the presence of gaseous or liquid H_2O. Water (vapor or liquid) enhances the capacity of carbon to catalyze SO_2 oxidation, but once a surface water film has formed, the transformation process is not highly dependent upon additional water. The transformation of SO_2 to sulfate by NO_2 on carbon does not appear to be inhibited at low pH.

References

[1] Calvert, J., FuSu, G., Bottenheim, J., and Strausz, O., "Mechanism of the Homogeneous Oxidation of Sulfur Dioxide in the Troposphere," *Atmospheric Environment*, Vol. 12, Jan.-March 1978, pp. 197-226.

[2] Hegg, D.A. and Hobbs, P.V., "The Homogeneous Oxidation of Sulfur Dioxide in Cloud Droplets," *Atmospheric Environment*, Vol. 13, July 1979, pp. 981-987.

[3] Penkett, S.A., Jones, B.M.R., Brice, K.A., and Eggleton, A.E.J., "The Importance of Atmospheric Ozone and Hydrogen Peroxide in Oxidizing Sulfur Dioxide in Cloud and Rainwater," *Atmospheric Environment*, Vol. 13, Jan. 1979, pp. 123-137.

[4] Novakov, T., Chang, S.G., and Harker, A.B., "Sulfates as Pollution Particulates: Catalytic Formation on Carbon (Soot) Particles," *Science*, Vol. 186, Oct. 1974, pp. 259-261.

[5] Chang, S.G. and Novakov, T., "Soot-Catalyzed Oxidation of Sulfur Dioxide," *Man's Impact on the Troposphere*, NASA RP-1022, Sept. 1978, pp. 349-369.

[6] Cofer, W.R. III, Schryer, D.R., and Rogowski, R.S., "The Enhanced Oxidation of SO_2 by NO_2 on Carbon Particulates," *Atmospheric Environment*, Vol. 14, May 1980, pp.571-575.

[7] Cofer, W.R. III, Schryer, D.R., and Rogowski, R.S., "The Oxidation of SO_2 on Carbon Particles in the Presence of O_3, NO_2, and N_2O," *Atmospheric Environment*, Vol. 15, June 1981, pp. 1281-1286.

[8] Rogowski, R.S., Schryer, D.R., Cofer, W.R. III, Munavalli, S., and Edahal, R.A. Jr., "Carbon Catalyzed Oxidation of SO_2 by NO_2 and Air," *Heterogeneous Atmospheric Chemistry* edited by D.R. Schryer, Vol 26, *Geophysical Monograph Series*, AGU Washington, Sept. 1982.

[9] Martin, R.L., Damschen, D.E., and Judeikis, H.S., "The Reactions of Nitrogen Oxides with SO_2 in Aqueous Aerosols," *Atmospheric Environment*, Vol. 15, Feb. 1981, pp. 191-195.

[10] "Standard Methods for Examination of Water and Wastewater," *Method* 427C, 14th Ed., published by American Public Health Association, Washington, D.C., 1975.

A Simple Model for Elastic Two-Dimensional Sails

P. S. Jackson*
Auckland University, Auckland, New Zealand

Introduction

THE flow around flexible lifting membranes (sails) is of interest because the equilibrium shape of the membrane emerges as part of the solution. The exact shape depends upon the pressure distribution on the surface, and this is turn depends upon the sail shape. The equations of fluid motion and sail equilibrium can be linearized if it is assumed that the sail camber and angle of attack are small, although Nielsen[1] and Thwaites[2] found that a numerical procedure was still required to solve the resulting "sail equation." It is shown here that quite good solutions can be obtained by assuming that the sail has a cubic shape. The standard results of thin-airfoil theory can then be combined with the conditions for force equilibrium on the sail to produce a relatively small set of equations. The equations are nonlinear and do not appear to have explicit solutions, except in some limiting cases, but they have the advantage that important variables like lift and sail tension appear directly. Numerical solutions are easily obtained, and are shown to be close to those obtained by Nielsen.[1]

The analysis is also extended to include the effects of sail stretch. This leads to a particular nondimensional combination of variables whose magnitude quantifies the relative significance of stretch, but it is found that the qualitative effects are quite predictable.

Simple Sail Model

A two-dimensional flexible membrane of length l is constrained by fixing its leading and trailing edges at the points $(0,b)$ and $(0,-b)$, as shown in Fig. 1. It then takes up an equilibrium shape under the action of an inviscid fluid whose freestream has dynamic pressure $\frac{1}{2}\rho V^2$, and makes an angle a with the horizontal axis. The forces acting on the membrane can thus be normalized by $\rho V^2 b$, giving coefficients C_L for the lift force and C_T for the tension in the sail.

The sail shape will usually be convex, but its details will depend upon the distribution of pressure along the surface. The pressure distribution depends in turn upon the details of the shape, but some of its overall effects are easily obtained from thin-airfoil theory. If the sail shape is assumed to be a cubic,

$$\frac{y}{b} = \frac{l}{4}\left(1 - \frac{x^2}{b^2}\right)\left(A + \frac{Bx}{b}\right) \tag{1}$$

then the theory gives for the coefficients of lift and leading-edge moment (from Ref. 4, p. 50)

$$C_L = 2\pi\left(a + \frac{A}{4} + \frac{B}{8}\right) \tag{2}$$

and

$$C_M = \pi\left(\frac{a}{2} + \frac{A}{4} + \frac{5B}{32}\right) \tag{3}$$

Received April 9, 1982. Copyright © American Institute of Aeronautics and Astronautics, Inc., 1982. All rights reserved.

*Senior Lecturer, Department of Mechanical Engineering.

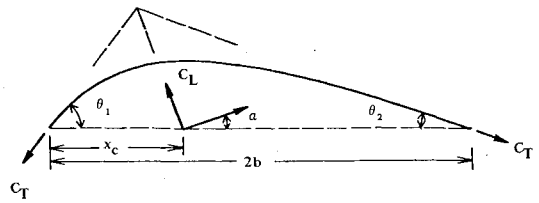

Fig. 1 Angles and forces on a two-dimensional sail.

It is more easily shown that $A=\theta_1+\theta_2$, $B=\theta_2-\theta_1$, so that these two parameters may be thought of as simple measures of the maximum camber and its position along the chord, respectively.

The sail length can be found by integrating along its surface,

$$l=\int_{-b}^{b}(1+\dot{y}^2)^{1/2}\,dx$$

Now, since the sail membrane is elastic its length depends upon the tension force. If a tension force T causes the sail length to increase by a fraction k then the length can also be written $2b(1+\epsilon)(1+kT)$, where $2b\epsilon$ is the initial excess of sail length over chord. Equating these two expressions, using Eq. (1) for $\dot{y}$ and expanding for small values of camber, leads to

$$\epsilon+\beta C_T=\frac{A^2}{24}+\frac{B^2}{40} \tag{4}$$

where

$$\beta=\rho U^2 bk$$

Two further equations can be obtained by considering the conditions for force equilibrium of the whole sail. Since the flow is inviscid there can be no drag force, and the resultant of the forces constraining the leading and trailing edges must balance the net lift force acting normal to the freestream. This is,

$$C_L=(C_T-C_F)\sin(\theta_1-a)+C_T\sin(\theta_2+a)$$

where C_F is the coefficient for the suction force which acts tangentially to the leading edge of the sail. Since C_F is of second order in a, when all the angles are small this equation reduces to

$$C_L=C_T A \tag{5}$$

Similarly, if the constraining forces are projected back along tangents to the leading and trailing edges they must intersect at a point through which the net lift also acts. Thus, if a line is drawn through this point normal to the freestream it intersects the chordline at the center of pressure. This construction leads to the exact result

$$\frac{x_c}{2b}=\frac{\tan\theta_2+\tan\theta_1\tan a}{\tan\theta_2+\tan\theta_1}$$

for the distance along the chord to the center of pressure. It may also be simplified when the angles are small, giving

$$\frac{x_c}{2b}=\frac{\theta_2}{\theta_2+\theta_1}=\frac{1}{2}+\frac{B}{2A} \tag{6}$$

Neither Thwaites[2] or Nielsen[1] seem to have noticed this result, which gives excellent predictions for x_c in the results given by Nielsen in his Table 2. Its importance here lies in the fact that a second expression for $x_c/2b$ can be obtained from Eqs. (2) and (3), since by definition this is the ratio of C_M to C_L. Equating the two expressions leads to

$$B^2+B[8a+(7A/4)]+4Aa=0 \tag{7}$$

This completes the necessary set of equations since, if ϵ, β, and a are known, there are five equations for the unknowns A, B, C_L, C_M, and C_T. These are Eqs. (2-5) and (7) which can be recast into the form

$$C_T,\ C_L/\sqrt{\epsilon}=\text{functions of } (a/\sqrt{\epsilon},\ \beta/\epsilon)$$

which for the case $\beta=0$ agrees with that obtained by Nielsen. The solutions to these equations when $\beta=0$ are compared with Nielsen's results in Fig. 2, where the agreement is seen to

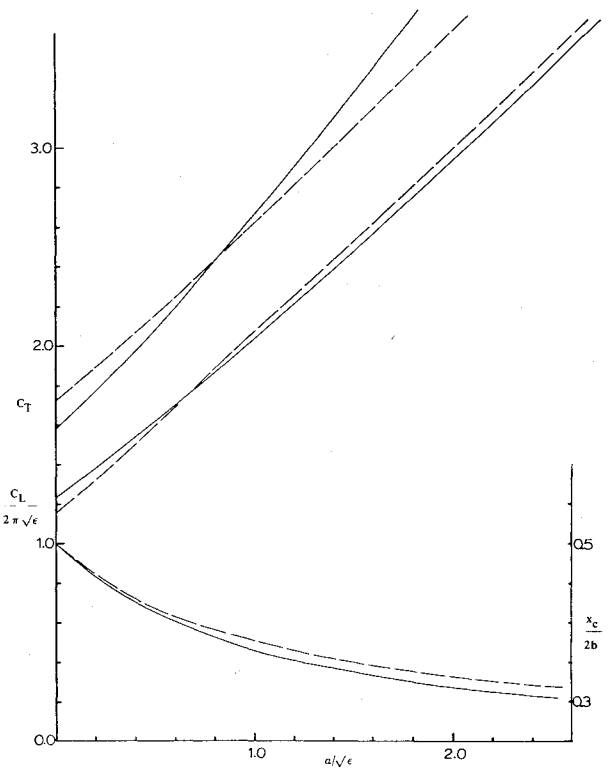

Fig. 2 A comparison of the simple model for no stretch (——) with Nielsen's exact solution (----); reduced lift and tension coefficients (left axis) and center of pressure (right) vs reduced angle of attack.

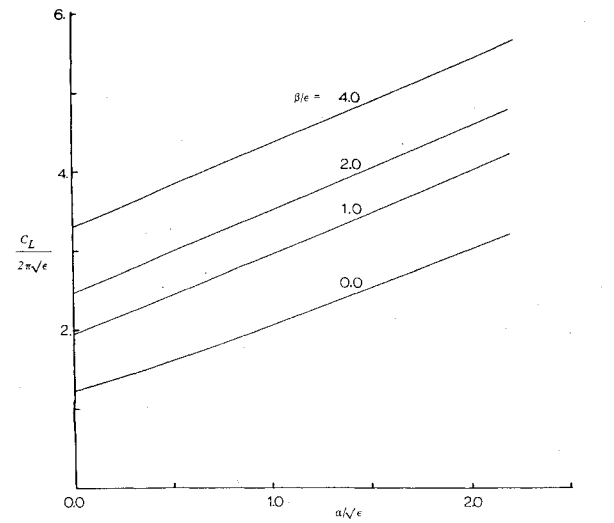

Fig. 3 Reduced lift coefficient vs reduced angle of attack, for various values of the stretch parameter β/ϵ.

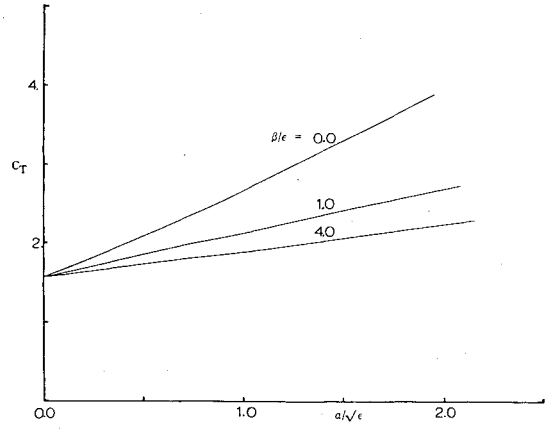

Fig. 4 Tension coefficient vs reduced angle of attack, for various values of the stretch parameter β/ϵ.

be very good. Additional solutions for various values of β/ϵ are given in Figs. 3 and 4. It can be seen that the effect of sail stretch is only to add greater camber, the general trends in C_L and C_T being quite predictable. For a given ϵ and a an elastic sail has more camber and lift than an inextensible sail, and less tension.

Asymptotic Solutions

A limiting case occurs when $a\sqrt{\epsilon}\to 0$, since then Eq. (7) gives $B=0$ so $\theta_1=\theta_2$ and the sail is symmetric in shape. The remaining equations reduce to

$$C_T=\pi/2, \qquad A=[24(\epsilon+\beta\pi/2)]^{1/2}, \qquad C_L=\pi A/2 \tag{8}$$

Thus the lift and camber increase with ϵ or β, but the tension always has a value of 1.57. When $\beta=0$ we find $C_L/\sqrt{\epsilon}=7.70$, compared with $C_L/\sqrt{\epsilon}=7.28$ and $C_T=1.73$ for the solution obtained by Nielsen. Irvine[3] also obtained $C_T=\pi/2$, assuming a circular arc profile. The solution for sails which are very stretchy or have no initial camber ($\epsilon/\beta\to 0$) is also interesting, in that at zero angle of attack $C_L/\sqrt{\beta}=9.64$, so that the lift force then has cubic dependence on speed U.

A second limit occurs when $B=-A/2$ since then the center of pressure arrives at the quarter-chord point, and the sail must resemble a flat plate. Equations (2) and (3) show that this requires that A/a and B/a vanish, when Eqs. (2) and (4) give

$$C_L=2\pi a, \qquad \epsilon+\frac{2\pi a\beta}{A}=\frac{A^2 23}{480}$$

Since $A/a\to 0$ the last equation only has meaning for the inextensible sail, $\beta=0$, when

$$A=(480\epsilon/23)^{1/2}, \; C_T\sqrt{\epsilon}/a=\pi(23/120)^{1/2}=1.375 \tag{9}$$

whereas Thwaites obtained 1.017 for the final number. The form for C_T shows that this case corresponds to that of very large tension and small camber, when the sail approaches the expected flat-plate shape. It is interesting to note the very small difference in magnitude between the values for A in the two limiting cases given by Eqs. (8) and (9) (for $\beta=0$). For any a it appears that the value of $C_L/\sqrt{\epsilon}C_T$ for an inextensible sail must lie in the range 4.57 to 4.90.

References

[1] Nielsen, J. N., "Theory of Flexible Aerodynamic Surfaces," *Journal of Applied Mechanics,* Vol. 30, Sept. 1963, pp. 435-442.

[2] Thwaites, B., "The Aerodynamic Theory of Sails," *Proceedings of the Royal Society,* Vol. A261, 1961, pp. 402-422.

[3] Irvine, H. M., "A Note on Luffing in Sails," *Proceedings of the Royal Society,* Vol. A365, 1979, pp. 345-347.

[4] von Kármán, T. and Burgers, J. M., "General Aerodynamic Theory," *Aerodynamic Theory,* Vol. 2, edited by W. F. Durand, Dover, New York, 1963.